Journal of Power Sources 222 (2013) 177–183

Contents lists available at SciVerse ScienceDirect

Journal of Power Sources

journal homepage: www.elsevier.com/locate/jpowsour

Short communication

Potassium carbonate as film forming electrolyte additive for lithium-ion batteries

Quan-Chao Zhuang*, Jia Li, Lei-Lei Tian

Lithium-ion Batteries Laboratory, School of Materials Science and Engineering, China University of Mining and Technology, No.8, South 3rd Ring Road, Quanshan District, Jiangsu, Xuzhou 221116, China

HIGHLIGHTS

- The performance of graphite anode is improved in $LiPF_6$–EC:DMC electrolyte with K_2CO_3.
- K_2CO_3 effectively suppresses the reduction of EC in the first lithiation process.
- The presence of K_2CO_3 modifies the morphology of SEI film to a worm mesh structure.
- This SEI is of better viscoelasticity to accommodate the volume changes of graphite.

ARTICLE INFO

Article history:
Received 11 April 2012
Received in revised form
9 August 2012
Accepted 17 August 2012
Available online 24 August 2012

Keywords:
Lithium-ion battery
Graphite electrode
Additive
Potassium carbonate

ABSTRACT

K_2CO_3 is evaluated as a film-forming additive in 1 mol dm^{-3} $LiPF_6$–EC:DMC electrolyte in lithium-ion batteries. It is found that the cyclic performance of graphite electrode is improved in the electrolyte with K_2CO_3, due to the reduction of EC during the first lithiation process is largely suppressed. Scanning electron microscopy (SEM) and electrochemical impedance spectroscopy (EIS) are used in order to better understand the reaction mechanism. The results show that, K_2CO_3 successfully modifies the SEI film to a worm mesh structure with better viscoelasticity to accommodate the volume changes of graphite electrode during electrochemical cycles, and makes it easier for lithium ions to intercalate into and deintercalate from the graphite electrode, thus contributes to better performance of graphite electrode.

1. Introduction

Lithium-ion batteries have been extensively used in a wide variety of portable electric devices such as mobile phones, laptops, electric vehicles, etc., owing to their high energy densities, long cycle life and environmental friendliness [1]. At present, graphite is the most widely adopted anode material in commercial lithium-ion batteries due to its high specific capacity, low working potential close to that of lithium metal, and superior cycling behavior [2]. It is generally known that during the first intercalation of lithium ions into the graphite electrode, the solvent and the lithium salt are reduced to form a surface film on graphite electrode which is commonly called the solid electrolyte interface (SEI) film. The formation of SEI film would inevitably lead to an irreversible capacity loss during the initial charge/discharge cycle of the lithium-ion cells [3]. However, the formed SEI film can prevent lithium ions from being intercalated in the solvated state, without which would otherwise lead to the exfoliation (swelling) of the carbon. In addition, the formed SEI film also prevents the electrolyte from being further reduced by the active lithium and thus limits the decomposition of the electrolyte [4,5].

Much research has been published on electrolyte additives because they play an important role in the formation of SEI films and have critical influences on the performance of lithium-ion batteries [6]. Up to now, many additives such as vinylene carbonate [7], ethylene sulfite [8], CO_2 [9] and SO_2 [10] have been proved to be effective in suppressing electrolyte decomposition reactions with different mechanisms. Tossici [11] found that KC_8, the compound of K^+ intercalated into the graphite layers, when used as electrode anode, had ideal charge/discharge behaviors and large rate capability. Choi et al. [12] studied the effect of CO_3^{2-} on graphite electrode and reported that adding appropriate amount of CO_3^{2-} in 1 mol dm^{-3} $LiPF_6$–EC:DMC could suppress the formation of $CH_3^{\bullet}$ radicals, reduce the total amount of hydrocarbons in the reduction products of electrolyte, consequently help to form a thin and dense SEI film on anode surface and reduce the first cycle

* Corresponding author. Tel.: +86 516 83591877; fax: +86 516 83591870.
E-mail address: zhuangquanchao@126.com (Q.-C. Zhuang).

0378-7753/$ – see front matter © 2012 Elsevier B.V. All rights reserved.
http://dx.doi.org/10.1016/j.jpowsour.2012.08.050

irreversible capacity loss. These results enlighten us that K_2CO_3, the combination of K^+ and CO_3^{2-}, which has the advantages of both K^+ and CO_3^{2-}, may be an effective film forming additive for lithium-ion batteries. However, Zheng et al. [13] reported the positive effects of K_2CO_3 in 1 mol dm^{-3} $LiClO_4$–EC:DEC electrolyte solution for enhancing the electrochemical performances of a natural graphite anode, but declared that it would only work in $LiClO_4$ based electrolyte.

In this present research, the electrochemical behaviors of graphite electrode in 1 mol dm^{-3} $LiPF_6$–EC:DMC electrolyte with and without K_2CO_3 were investigated using charge/discharge tests and cyclic voltammograms. The SEI morphology and structure were characterized by SEM. To elaborate the possible mechanisms of the enhanced performances of graphite electrode in the electrolyte containing K_2CO_3 as an additive, EIS measurement was applied, the obtained data were fitted using Zview software, and variations of kinetics parameters with electrode polarization potential were analyzed.

2. Experimental

The graphite electrodes used in this study were prepared by spreading a mixture of 90% mesocarbon microbeads (MCMB, Beiterui new energy materials Co., Shenzhen China) and 10% ployvinylidene fluoride (Kynar FLEX 2801, Elf-atochem, USA) binder dissolved in *N*-methyl pyrrolidone (Fluka Inc.) onto a piece of Cu foil (thickness: 20 μm) current collector. The solvent was removed by baking at 120 °C under vacuum. The foil was then cut into 1 cm^2 circle and 2 × 4 cm^2 rectangular plates as the electrodes for half cell and three-electrode cell, respectively. The dried electrodes were compressed by a roller at room temperature to make a smooth and compact structure.

The electrolyte was 1 mol dm^{-3} $LiPF_6$ in a mixture of ethylene carbonate (EC) and dimethyl carbonate (DMC) (1:1, weight ratio, Guotaihuarong Co., Zhangjiagang, China). Before using, additive K_2CO_3 was dried under vacuum at 80 °C for 24 h. Afterward, proper amount of K_2CO_3 was added in 1 mol dm^{-3} $LiPF_6$–EC:DMC electrolyte in a glove box under argon atmosphere and shook fully to obtain saturated solution. The estimated amount of K_2CO_3 in the electrolyte is 1.2 g L^{-1}, measured by gravimetric method.

The charge/discharge experiments were conducted in half cells using Li foil (99.9%, China Energy Lithium Co., Ltd., Tianjin, China) as counter electrode. The cells were galvanostatically charged and discharged at a current density of 30 mA g^{-1} over the range of 0–3 V. The CV and EIS measurements were performed in three-electrode cells with Li foils served as both the auxiliary and reference electrodes on an electrochemical work station (CHI 660C, Chenhua Co., Shanghai, China). The CV curves were measured at 1 mV s^{-1} over the range from 3 V to 0 V. After CV cycling, the graphite electrode was washed in DMC solution and dried under vacuum to remove the residual electrolyte for SEM observation. The amplitude of the ac perturbation signal was 5 mV and the frequency range varied from 10^5 to 10^{-2} Hz. The electrode was equilibrated for 1 h before EIS measurements to attain a steady condition of sufficiently low residual current. The impedance results obtained were fitted using Zview software. All the potentials indicated here were referenced to the Li/Li$^+$ electrode potential.

3. Results and discussion

3.1. Electrochemical performance

The charge/discharge curves and cyclic performance of the graphite electrode in electrolytes with and without K_2CO_3 are displayed in Figs. 1 and 2, respectively. The discharge capacity of

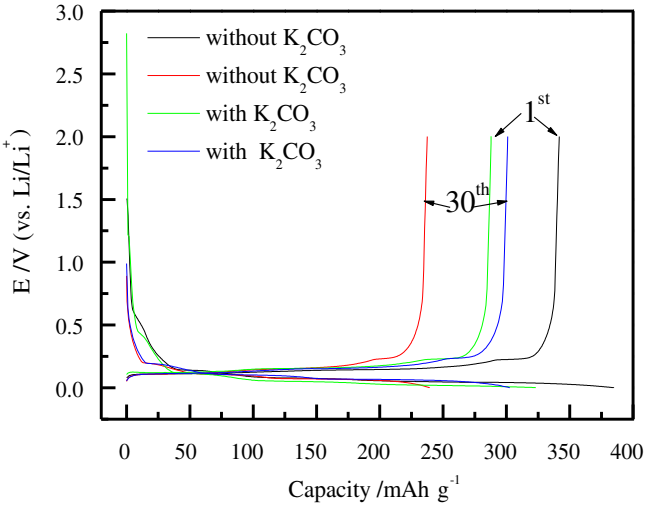

Fig. 1. The 1st and the 30th charge/discharge curves in 1 mol dm^{-3} $LiPF_6$–EC:DMC electrolyte without and with K_2CO_3.

graphite at the 1st and the 30th circle in K_2CO_3 free electrolyte is 385 mA h g^{-1} and 239 mA h g^{-1}, respectively, and the capacity retention is only 62.2% after the 30th cycle. When the graphite electrode is cycled in the electrolyte containing K_2CO_3, the discharge capacity at the 1st circle is 323 mA h g^{-1}, slightly smaller than that in the electrolyte without K_2CO_3. However, during the first 7 circles, the discharge capacity increases gradually with the circle number, and reaches 343 mA h g^{-1} at the 7th circle, afterward the capacity drops slowly. After the 30th circle, the discharge capacity is 303 mA h g^{-1} and an excellent capacity retention of 93.7% is maintained, much higher than that in the K_2CO_3 free electrolyte, indicating that the cyclic performance of graphite electrode is improved significantly in the electrolyte containing K_2CO_3.

Cyclic voltammograms of graphite electrodes in electrolytes with and without K_2CO_3 are presented in Fig. 3. For the graphite electrode in K_2CO_3 free electrolyte, three peaks are observed during the first cathodic sweep. Peak I appears at the voltage around 0.7 V and peak II around 0.4 V. These two peaks disappear completely during the subsequent cycles, indicating that peaks I and II are

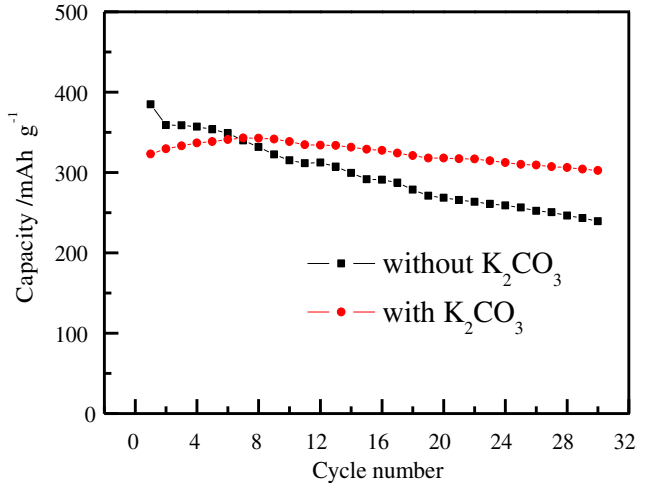

Fig. 2. Cyclic performance of graphite electrode in 1 mol dm^{-3} $LiPF_6$–EC:DMC electrolyte without and with K_2CO_3.

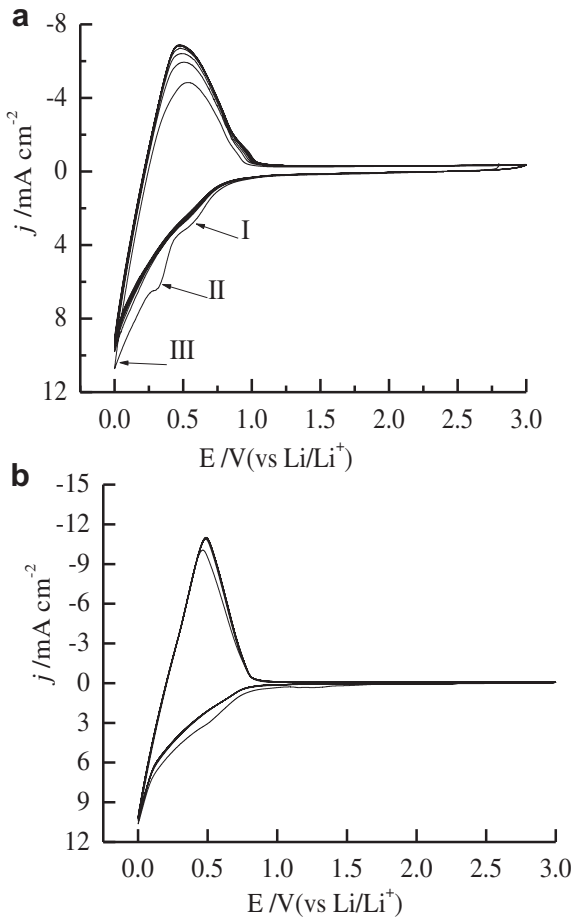

Fig. 3. Cyclic voltammograms (CVs) of the graphite electrode in 1 mol dm^{-3} $LiPF_6$–EC:DMC electrolyte: (a) without and (b) with K_2CO_3.

attributed to the formation of SEI film. According to Naji et al.[14] the reduction process of EC mainly includes two steps.

The first step (single electron reduction process):

$$EC + 2e^- + 2Li^+ \rightarrow Li_2CO_3 + C_2H_4 \quad (1)$$

The second step (double electrons reduction process):

$$EC + e^- + Li^+ \rightarrow \left[Li^+EC\right]^- \quad (2)$$

$$2\left[Li^+EC\right]^- \rightarrow (-CH_2OCO_2Li)_2 + C_2H_4 \quad (3)$$

$$2\left[Li^+EC\right]^- \rightarrow (-CH_2CH_2OCO_2Li)_2 \quad (4)$$

Thus, it can be proposed that peak I is attributed to the reduction of EC into Li_2CO_3, and peak II is associated with EC reduced into alkyl lithium carbonate. The peak at 0 V is characteristic of lithium ions intercalation into the lattice of the graphite electrode. The anodic peak at around 0.5 V is ascribed to the corresponding deintercalation of lithium ions [15]. Furthermore, the small broad reduction peak observed between 1.5 V and 1.0 V during the first cathodic sweep may be ascribed to the reduction of impurities [16,17].

For the graphite electrode in the electrolyte containing K_2CO_3, in the first cathodic process, it is interesting to see that only the peak corresponding to lithium ions intercalation process appears, peaks related to EC reduction process are no longer to be observed, illustrating that the reduction of EC during the first lithiation process is largely suppressed. In subsequent circles, the CV curves show a high degree of overlap, and the currents of both the intercalation and deintercalation peak remain almost unchanged, indicating that the cyclic performance of graphite electrode in the electrolyte containing K_2CO_3 is much better than that in the K_2CO_3 free electrolyte, corresponding to the charge/discharge results.

3.2. Characterization of graphite electrode surface

To gain more information about the surface morphology of the graphite electrode, SEMs of the graphite electrode before and after cycling in electrolyte without and with K_2CO_3 are shown in Figs. 4–6. It is seen that the MCMB used in our study has a spherical graphite form with particle size about 5–20 μm, and has a relatively smooth surface before electrochemical cycling. After 10 CV circles, a thin SEI layer adhering to the active material surface is observed in both electrolyte with and without K_2CO_3. According to previous researches [18,19], the major components of SEI film are the reduction products of electrolytes, such as Li_2CO_3, LiF, $(CH_2OCO_2Li)_2$, $ROCO_2Li$. The SEI film formed in K_2CO_3 free electrolyte is composed of spherical particles about 20 nm and there are obvious cracks on the surface of SEI film. But in electrolyte with K_2CO_3, the structure of the formed SEI film is completely different from that in the K_2CO_3 free electrolyte. The graphite particles gather and form a well-organized warm mesh pattern. In addition, the cracks are no longer to be seen on the SEI film surface, indicating the addition of K_2CO_3 in the electrolyte successfully modifies the morphology of SEI film on the graphite surface. According to D. Aurbach [20], the formation of cracks in the surface of SEI would lead to further reaction of the active surface with solution species. Although occurring only on a small scale, the breakdown and repair of SEI films would lead to a gradually thickening of the SEI, hence to an increase in the electrode's impedance. Thus it is speculated that this porous network structure may provide the SEI film with better viscoelasticity to accommodate the volume changes of graphite electrode during electrochemical cycles, as a result contributes to the enhanced cyclic performance of lithium-ion battery, which is consistent with the above CV and charge/discharge results.

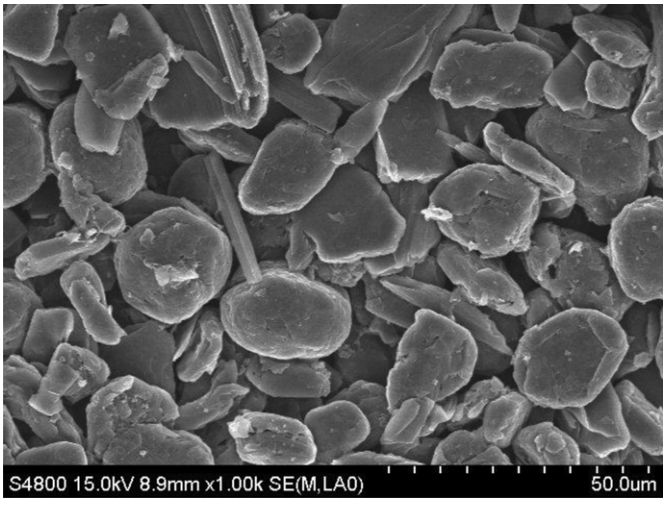

Fig. 4. SEM image of graphite electrode before CV cycle.

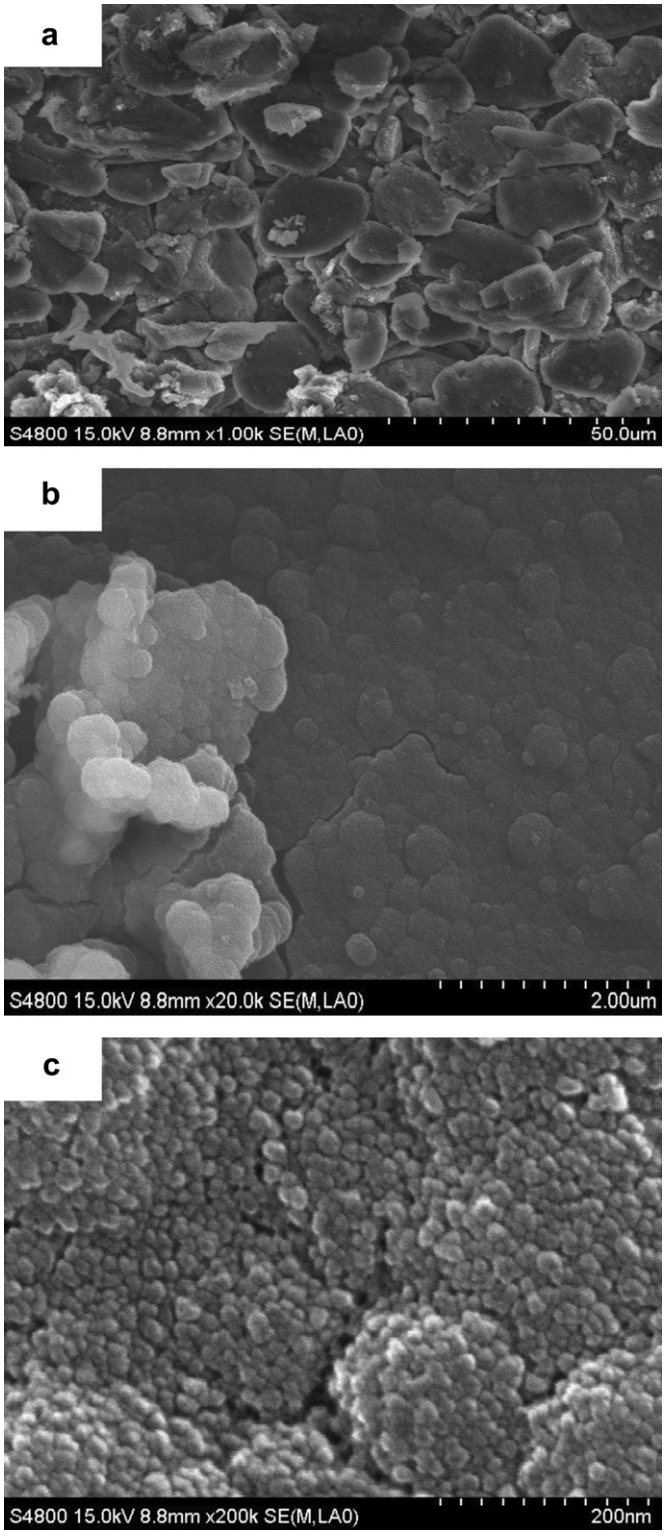

Fig. 5. SEM images of graphite electrode after CV cycle in the electrolyte without K_2CO_3 under different magnification: (a) 1.00K times; (b) 20.0K times; (c) 200K times.

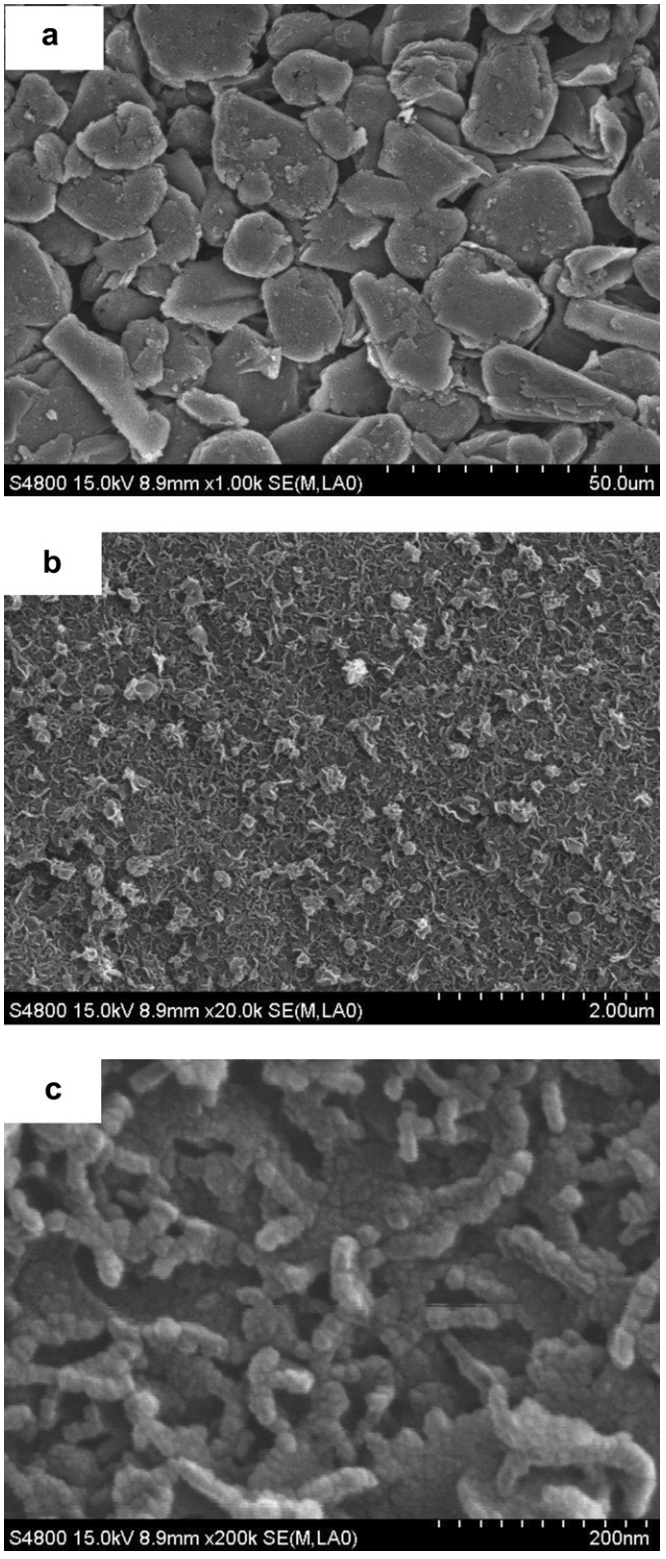

Fig. 6. SEM images of graphite electrode after CV circle in the electrolyte with K_2CO_3 under different magnification: (a) 1.00K times; (b) 20.0K times; (c) 200K times.

3.3. Characterization of EIS

The electrochemical impedance spectroscopy (EIS) technique has been proved to be an effective method to study the electrode reaction mechanism of lithium batteries [21–24]. To further explore the reason for improvement of K_2CO_3 on the electrochemical performance of graphite electrodes, the impedance behaviors of graphite electrodes are recorded. The Nyquist plots of graphite electrodes in the electrolytes with and without K_2CO_3 at different potentials during the course of lithium ions intercalation are plotted in Fig. 7. At the open circuit potential

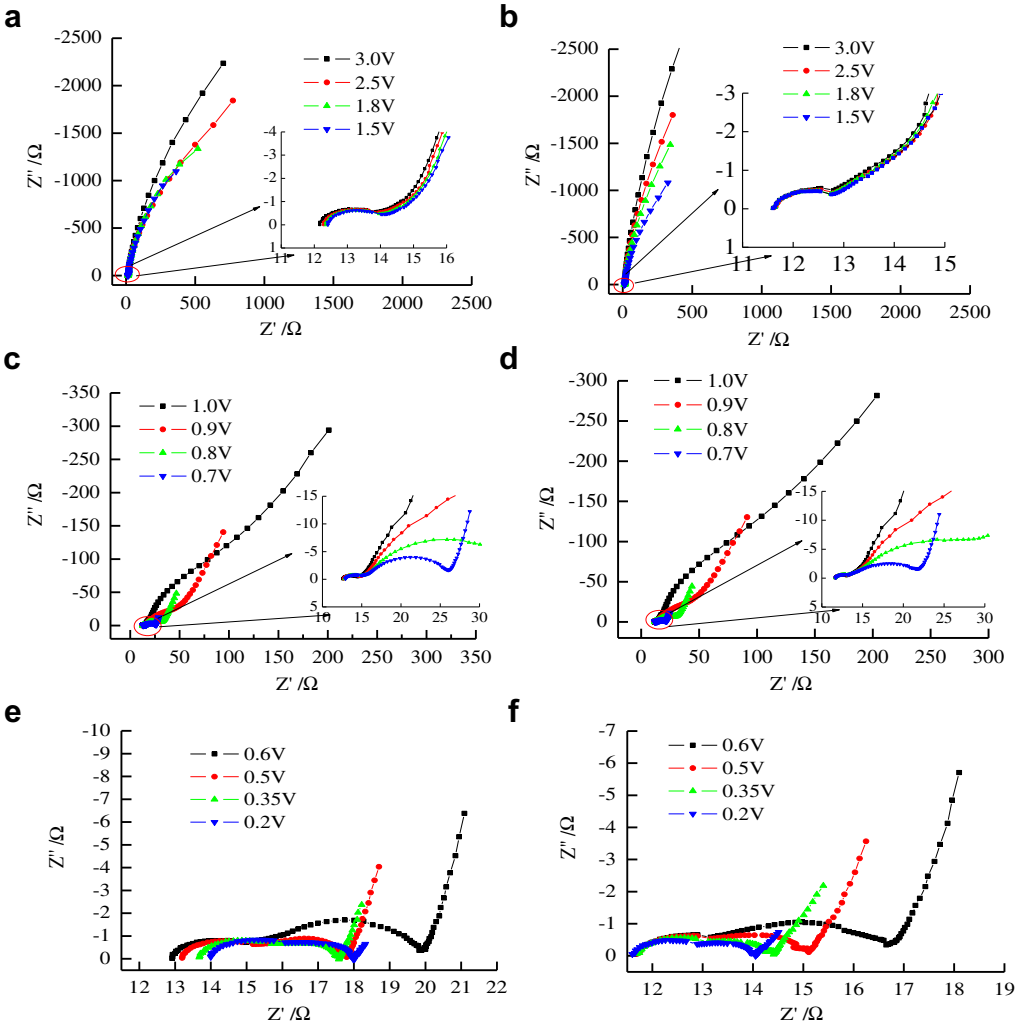

Fig. 7. Nyquist diagrams of the graphite electrode at various potentials from 3.0 to 0.2 V in the first discharge process in the electrolyte: (a), (c), (e) without K_2CO_3; (b), (d), (f) with K_2CO_3.

(3.0 V), the EIS curves are similar to each other, both show a small high-frequency semicircle and an arc in low frequency region. Because there is no SEI film before electrochemical circle, the high-frequency semicircle should be attributed to the contact problems, as suggested by Holzapfel et al. [25], while the low-frequency arc reflects the retardance characteristic of graphite electrode [26]. When the potential drops to 1.0 V, the Nyquist graphs in both electrolytes are consisted of 3 parts, namely high-frequency arc (HFA), middle-frequency arc (MFA), and a line in the low frequency range. According to previous researches [20,27–31], the HFA is commonly attributed to the process of lithium ions migrating through SEI film, the MFA is ascribed to charge transfer process at the electrolyte–electrode interface while the sloping line at low frequency is a reflection of lithium ion solid-state diffusion within the graphite electrode. Considering the truth that there has been an initial semicircle in the high frequency region when the potential is higher than 1.2 V, we propose that the HFA in this study is related to both the contact problems and the migration of lithium ions migration through the SEI film.

Based on the above analysis, an equivalent circuit, as shown in Fig. 8, is proposed to fit the impedance spectra of the graphite electrode during the first lithiation process. In this equivalent circuit, R_s represents the ohmic resistance, while R_{SEI} and R_{ct} are resistances of the SEI film and the charge transfer reaction, respectively. The capacitances of the SEI films and the double layer are represented using the constant phase elements (CPE) Q_{SEI} and Q_{dl} respectively. Considering the fact that the low frequency region cannot be modeled properly using the finite Warburg element, we use a CPE instead, i.e. Q_D. This method has been successfully used to characterize the graphite electrodes [32], and can make it possible for us to obtain a good match with the experimental data. The expression for the admittance response of the CPE (Q) is:

$$Y = Y_0\omega^n \cos\left(\frac{n\pi}{2}\right) + jY_0\omega^n \sin\left(\frac{n\pi}{2}\right) \quad (5)$$

In this equation, ω is the angular frequency, j is the imaginary unit and n stands for the disperse coefficient. A CPE represents

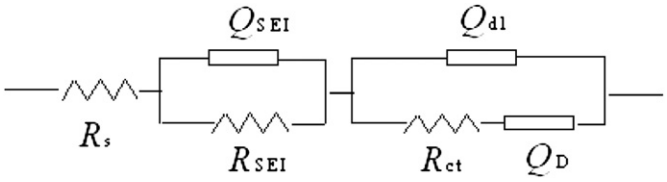

Fig. 8. Equivalent circuit proposed for analysis of the graphite electrode in the first charge/discharge process.

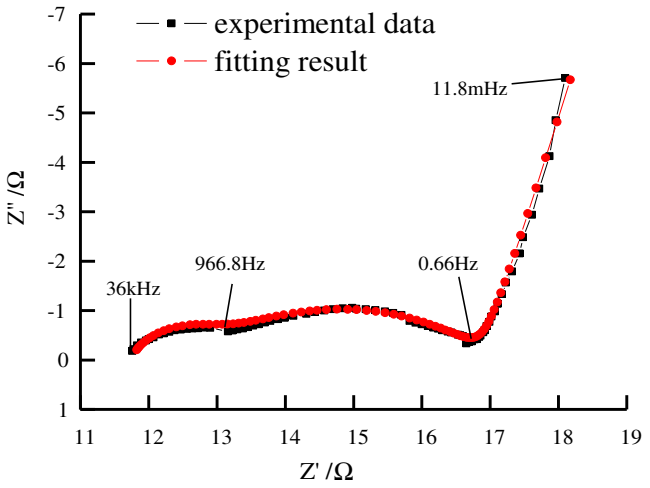

Fig. 9. A comparison of EIS data and fitting result at 0.6 V using equivalent circuit in Fig. 8.

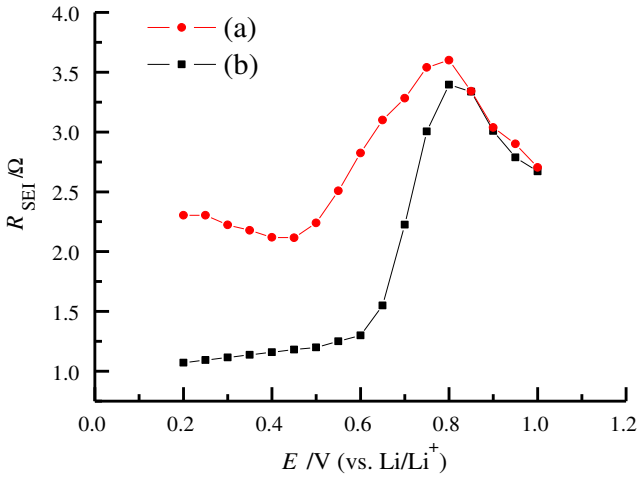

Fig. 10. Variation of R_{SEI} with the electrode potential in the electrolyte: (a) without K_2CO_3; (b) with K_2CO_3.

a resistor when $n = 0$, a capacitor with capacitance of C when $n = 1$, an inductor when $n = -1$, and a Warburg resistance when $n = 0.5$.

The equivalent circuit in Fig. 8 can satisfactorily describe the EIS data at different potentials. Fig. 9 shows a typical fitting result compared with the experimental EIS data at 0.6 V in the first discharge process, and the values for all the related parameters fitted are listed in Table 1 As can be seen, the relative standard deviations of most parameters obtained are within 15%.

3.4. Variation of R_{SEI} with the electrode polarization potential

Fig. 10 illustrates the variations of R_{SEI} obtained by fitting the experimental impedance spectra of the graphite electrode during the course of lithium ions intercalation process with the electrode polarization potential in the electrolytes with and without K_2CO_3. In K_2CO_3 free electrolyte, over the range of 1.0–0.8 V, R_{SEI} increases with the decreasing electrode polarization potential, indicating the SEI film begins to form and grow thicker. During the potential of 0.8–0.45 V, R_{SEI} decreases with the decrease of electrode polarization potential, which may be ascribed to that the reduction products of EC, such as alkyl lithium carbonate, react with the trace amount of water to form a composition with better lithium ion conducting property [33]. On further charging to 0.2 V, the SEI resistance increases with the decrease of electrode polarization potential, this may be ascribed to the phenomenon that lithium ion begins to intercalate into the graphite electrode in large quantity below 0.4 V, which leads to an inevitable inflation of graphite particles. However the SEI film formed in K_2CO_3 free electrolyte is not viscoelastic enough to accommodate with the tiny volume changes of graphite particles during lithium ions intercalation process, thus results in the cracking of the SEI film. Subsequently, the active masses react with the electrolyte solution species to repair the cracking of the SEI film. The above cracking and repairing of the SEI film lead to an increase in the R_{SEI} [34,35]. In electrolyte containing K_2CO_3, on charging from 1.0 to 0.8 V, variations of the resistance of SEI film have a similar trend. However, during the following cathodic polarization below 0.8 V, R_{SEI} keeps decreasing, implying that the presence of K_2CO_3 can improve the viscoelasticity of SEI film to better accommodate with the volume changes during lithium ions intercalation process, and the cracking and repairing of the SEI film are avoided.

Table 1
Equivalent circuit parameters of Nyquist simulation results in the first discharge cycle at 0.6 V.

Element	Value	Error%
R_S	11.72	0.61246
Q_{SEI}–Y_0	0.00014851	10.501
Q_{SEI}–n	0.87979	39.303
R_{SEI}	1.103	5.1303
R_{ct}	4.107	3.0728
Q_{dl}–Y_0	0.00042886	4.214
Q_{dl}–n	0.014774	2.5665
Q_D–Y_0	0.026508	1.6403
Q_D–n	0.0061003	0.70988

3.5. Variation of ln R_{ct} with electrode polarization potential

Fig. 11 presents the fitting results of R_{ct} and ln R_{ct} varying with the electrode potential in the electrolytes without and with K_2CO_3. According to our previous work [36,37],

$$R_{ct} = \frac{RT}{n^2F^2c_T k_0 (M^+)^{(1-\alpha)}} \exp[-\alpha f(E - E_0)] \quad (6)$$

Here n is the number of electrons exchanged during the charge and discharge process, R and F represent the thermodynamic and Faraday constant each, while α represents the symmetry factor of the electrochemical reaction, $f = F/RT$, E and E_0 are the electrode's real and standard potentials respectively. M^+ stands for the concentration of lithium ions in the electrolyte near the electrode, and c_T (mol cm^{-3}) is the maximum concentration of lithium-ions in graphite electrode, k_0 is the standard reaction rate constant.

After using a logarithm to linearize equation (6), we can obtain the following equation:

$$\ln R_{ct} = \ln \frac{RT}{n^2F^2c_T k_0 (M^+)^{(1-\alpha)}} - \alpha f(E - E_0) \quad (7)$$

From equation (7), we know if $x \to 0$, ln R_{ct} and E will have a linear relationship. The symmetry factor α can be calculated from the slope. It can be seen that ln R_{ct} varies linearly with the electrode polarization potentials between 0.5 V and 1.0 V during the first lithium-ion intercalation process in both electrolytes, implying that equation (7) can be used to properly interpret the experimental data and α in the electrolyte with and without K_2CO_3 is determined to be 0.167 and 0.175, respectively. Moreover, R_{ct} in the electrolyte

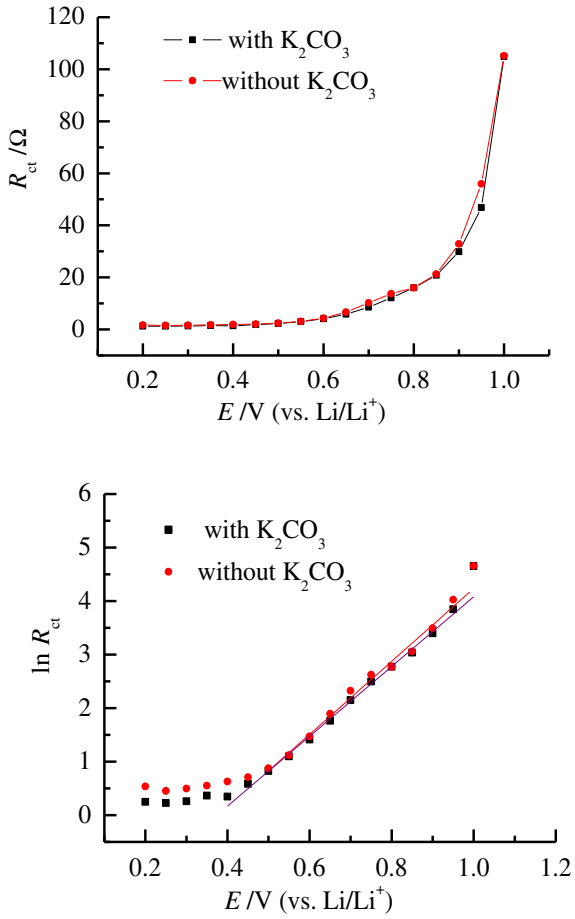

Fig. 11. Variations of R_{ct} and ln R_{ct} with the electrode polarization potential in the electrolyte without and with K_2CO_3.

containing K_2CO_3 is smaller than that in the K_2CO_3 free electrolyte below 0.4 V, indicating that it is easier for lithium ions to intercalate into and deintercalate from the graphite electrode in the electrolyte containing K_2CO_3.

4. Conclusions

The positive effects of K_2CO_3 on the electrochemical behaviors of graphite electrode in 1 mol dm^{-3} $LiPF_6$–EC:DMC electrolyte are confirmed by SEM, charge/discharge test, cyclic voltammetry, and EIS measurements. The charge/discharge and CV studies reveal that the presence of K_2CO_3 can effectively suppress the reduction of EC during the first lithiation process. The SEM images indicate that, the porous network structure of SEI film formed in electrolyte added K_2CO_3 is advantageous to lithium ion batteries. EIS results indicate that K_2CO_3 can keep the resistance of SEI film from growing larger, improve the viscoelasticity of SEI film. All these effects seem to contribute to the improved cyclic performance of graphite electrode. We believe these favorable effects may help the development of improved additives for enhanced lithium-ion battery performance.

Acknowledgments

This work was supported by the Fundamental Research Funds for the Central Universities (2010LKHX03).

References

[1] J.A. Carpenter, J. Gibbs, A.A. Pesaran, et al., MRS Bull. 33 (2008) 439.
[2] H.H. Zheng, K. Jiang, T. Abe, Z. Ogumi, Carbon 44 (2006) 203.
[3] D. Aurbach, Y. Ein-Eli, O. Cfusid, J. Electrochem. Soc. 141 (1994) 603.
[4] J.S. Kim, Y.T. Park, J. Power Sources 91 (2000) 172.
[5] M. Stjerndahl, H. Bryngelsson, T. Gustafsson, et al., Electrochim. Acta 52 (2007) 4947.
[6] S.S. Zhang, J. Power Sources 162 (2006) 1379.
[7] D. Aurbach, K. Gamolsky, B. Markovsky, et al., Electrochim. Acta 47 (2002) 1423.
[8] G.H. Wrodnigg, J.O. Besenhard, M. Winter, J. Electrochem. Soc. 146 (1999) 470.
[9] M.D. Levi, E. Markevich, C. Wang, et al., J. Electrochem. Soc. 151 (2004) A848.
[10] Y. Ein-Eli, S. Thomas, R. Koch, J. Electrochem. Soc. 144 (1997) 1159.
[11] R. Tossici, M. Berrettoni, M. Rosolen, et al., J. Electrochem. Soc. 143 (1996) L64.
[12] Y.K. Choi, K. Chung, W.S. Kim, et al., J. Power Sources 104 (2002) 132.
[13] H.H. Zheng, Y.B. Fu, Electrochem. Solid-State Lett. 9 (2006) A115.
[14] A. Naji, J. Ghanbaja, B. Humbert, et al., J. Power Sources 63 (1996) 33.
[15] O. Chusid, Y. Ein-Eli, D. Aurbach, et al., J. Power Sources 43 (1993) 47.
[16] J. Felix, R. Beat, I. Roman, et al., J. Power Sources 81–82 (1999) 243.
[17] D. Aurbach, I. Weissman, A. Zaban, P. Dan, Electrochim. Acta 45 (1999) 1135.
[18] R. Fong, U.V. Sacken, J.R. Dahn, et al., J. Electrochem. Soc. 137 (1990) 2009.
[19] Z.X. Shu, R.S. Mcmilan, J.J. Murray, et al., J. Electrochem. Soc. 140 (1993) 922.
[20] D. Aurbach, J. Power Sources 89 (2000) 206.
[21] N. Dimov, K. Fukuda, T. Umeno, et al., J. Power Sources 114 (2003) 88.
[22] X.W. Zhang, C. Wang, A.J. Appleby, J. Power Sources 114 (2003) 121.
[23] Y.Q. Chu, Z.W. Fu, Q.Z. Qin, Electrochim. Acta 49 (2004) 4915.
[24] W.C. Choi, D. Byun, J.K. Lee, et al., Electrochim. Acta 50 (2004) 523.
[25] M. Holzapfel, A. Martinent, F. Allion, et al., J. Electroanal. Chem. 546 (2003) 41.
[26] Y.C. Chang, H.J. Sohn, J. Electrochem Soc. 147 (2000) 50.
[27] M.D. Levi, D. Aurbach, J. Phys. Chem. B 109 (2005) 2763.
[28] M.D. Levi, D. Aurbach, J. Phys. Chem. B 101 (1997) 4630.
[29] D. Aurbach, M.D. Levi, E. Levi, et al., J. Electrochem. Soc. 145 (1998) 3024.
[30] D. Aurbach, K. Gamolsky, B. Markovsky, et al., J. Electrochem. Soc. 147 (2000) 1322.
[31] B. Markovsky, M.D. Levi, D. Aurbach, Electrochim. Acta 43 (1998) 2287.
[32] Q.C. Zhuang, Z.F. Chen, Q.F. Dong, et al., Chin. Sci. Bull. 51 (2006) 17.
[33] L.L. Tian, Q.C. Zhuang, et al., Chem. J. Chin. Univ. C 31 (2010) 2468.
[34] C. Wang, I. Kakwom, A.J. Appleby, et al., J. Electroanal. Chem. 489 (2000) 55.
[35] C. Wang, A.J. Appeleby, F.E. Litlle, J. Electroanal. Chem. 497 (2001) 33.
[36] S.D. Xu, Q.C. Zhuang, L.L. Tian, et al., J. Phys. Chem. 115 (2011) 9210.
[37] L.L. Tian, Q.C. Zhuang, J. Li, et al., Chin. Sci. Bull. 56 (2011) 3204.